

Numerical Simulation of Mass Transfer Aiming at Food Processes and Bioprocesses in Fixed-Bed Equipment: a Comparison Between Finite-Differences and Lattice-Boltzmann Method

JOSÉ A. RABI

Faculty of Animal Science and Food Engineering (FZEA), University of São Paulo (USP)
Av. Duque de Caxias Norte 225, 13635-900, Pirassununga, SP
BRAZIL

jrabi@usp.br <http://www.usp.br/fzea/>

Abstract: - Lattice-Boltzmann method (LBM) has been alternatively used to numerically simulate mass transfer in porous media. Supercritical fluid extraction (SFE) and biospecific affinity chromatography (BAC) are fixed-bed processes that may benefit from LBM as their model frameworks are very similar. By allowing the species concentration in the fluid phase to vary both in time and along the bed axis, this work has simplified SFE and BAC models in order to obtain an identical governing partial differential equation (PDE). Cast in dimensionless form, such mutual PDE was numerically solved through either LBM or finite-differences method (FDM). As far as false diffusion is concerned, numerical simulations were compared and results encourage the use of LBM as a simulation tool to investigate either SFE or BAC processes.

Key-Words: - mass transfer, fixed bed, porous media, numerical simulation, finite-differences method, lattice-Boltzmann method

1 Introduction

One may rely on distinct modeling approaches in order to simulate transport phenomena, with models varying between the following extremes [1]: from physics-based to data-driven, from deterministic to stochastic, from macroscopic to microscopic, and from analytical to numerical. “Combinations” are allowed as one may propose, for instance, physics-based models in either macroscopic, mesoscopic or microscopic scales [2]. In effect, one may use any scale to simulate transport phenomena within porous media [3], which is the case of those involving food or bioproducts. Although comprehensive models for food or bioprocesses may result complex [4], their numerical simulation has continuously increased as computational tools have been developed [5] while their importance have been recognized [6].

With widespread use for food or bioprocesses, macroscopic modeling leads to partial differential equations (PDEs) for observable properties (e.g. species concentration and temperature). As systems contain a huge number of particles, such properties are interpreted as average values at a point in the continuum. On the opposite end, the microscopic approach considers each single constituent particle, identified together with inter-particle interactions to be used in Newton’s law of motion. Referred to as molecular dynamics (MD), the resulting simulation requires large computational effort [3].

Lying between the two later modeling levels, the mesoscopic approach deals with global effects of particle via a so-called distribution function, which attempts to depict the behavior of a relatively small particle collection. Based on such function, lattice-Boltzmann method (LBM) is implemented so that one may distinguish it from both MD simulation and classical macroscale discretization methods such as finite-differences (FDM), finite-volumes (FVM) and finite-elements (FEM) [7].

In LBM, bulk medium is treated as a collection of constituent particles occupying a discrete space (lattice sites). During a discrete time lag, particles travel between sites along pre-defined directions (lattice links). When they arrive at adjacent sites, particles mutually collide and are rearranged. Such dynamics is described by two LBM steps referred to as “streaming” and “collision”. By assuming that such dynamics obeys basic conservation principles while being isotropic, LBM may properly describe and simulate macroscopic medium behavior [8].

Being a discrete approach for the kinetic theory, LBM has been applied to food and bioprocesses and simulated systems have included (but not restricted to) flows in porous media, colloidal suspensions, polymer solutions and emulsions [9]. The present work aims at LBM simulation of biospecific affinity chromatography (BAC) as well of supercritical fluid extraction (SFE) in fixed bed equipment. Even when

model simplifications are evoked, inherent hurdles still justify the use of numerical methods to simulate either BAC or SFE processes.

2 Theory

2.1 Models for BAC and SFE processes

Fixed-beds considered in this work are cylinders of inner radius R and length L , either horizontally or vertically oriented as shown in Fig. 1. Bed inlet is at $z = 0$ while outlet is at $z = L$, with respect to fluid flow. In BAC the later is the percolating solution whereas in SFE it refers to the supercritical fluid. Porosity ϵ is allegedly uniform throughout the bed.

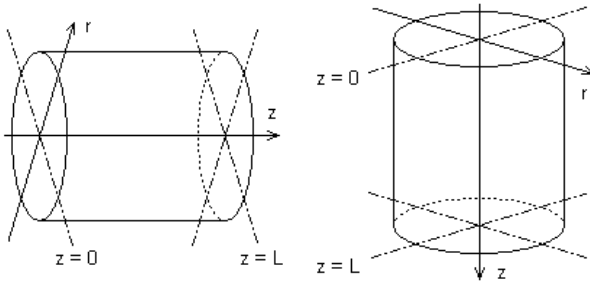


Fig. 1. Cylindrical coordinates (r - z) for fixed-beds considered in the present work.

If the volumetric flow rate \dot{V} remains constant, the interstitial velocity $v_z = \dot{V}/(\epsilon\pi R^2)$ is uniform. In model equations, one may use the so-called seepage velocity $\tilde{v}_z = \dot{V}/(\pi R^2)$ instead [10]. The idea when assessing velocities \tilde{v}_z and v_z is depicted in Fig. 2, being $A = \pi R^2$ bed total cross-sectional area while $A_f = \epsilon A$ and $A_s = (1-\epsilon)A$ are those occupied by fluid and solid phases, respectively.

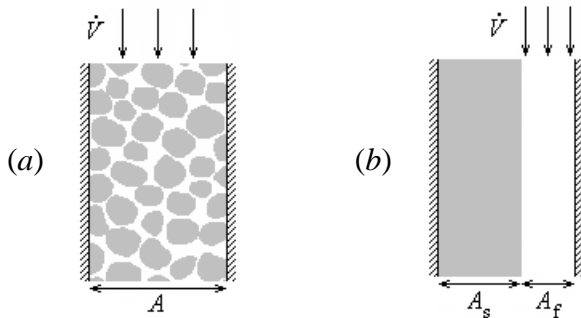


Fig. 2. Evaluation of (a) seepage velocity $\tilde{v}_z = \dot{V}/A$ and (b) interstitial velocity $v_z = \dot{V}/A_f = \dot{V}/(\epsilon A)$.

BAC models have evoked uniform fluid flow, sorption-desorption kinetics and species transport by convection and/or diffusion [11]-[17]. Those models have been of first-order with respect to the spatial dependence so that species concentrations may vary along a given coordinate z (i.e., fixed-bed axis), apart from depending on time t . Such concentrations have then been modeled as $\phi = \phi(z,t)$ and $\theta = \theta(z,t)$ in fluid and solid phases, respectively, and related governing PDEs have been expressed as:

$$\frac{\partial \phi}{\partial t} + v_z \frac{\partial \phi}{\partial z} = D_z \frac{\partial^2 \phi}{\partial z^2} - \frac{1-\epsilon}{\epsilon} \dot{r} \quad (1)$$

$$\frac{\partial \theta}{\partial t} = \dot{r} = k_1 \phi (\theta_{\max} - \theta) - k_2 \theta \quad (2)$$

where D_z is species axial diffusivity, k_1 and k_2 are respectively sorption and desorption coefficients and θ_{\max} is the maximum adsorption capacity of the chromatographic column. Giving the rate at which species are adsorbed from fluid to solid phase, term \dot{r} behaves as a sink in Eq. (1) and as a source in Eq. (2). As initial conditions, one may prescribe:

$$\text{at } t = 0: \phi = 0 \text{ and } \theta = 0 \quad (3)$$

while boundary conditions might be:

$$\text{at } z = 0: \phi = \phi_{\text{in}} \quad ; \quad \text{at } z = L: \frac{\partial \phi}{\partial z} = 0 \quad (4)$$

being $\phi_{\text{in}} \neq 0$ a known inlet concentration.

SFE models have equally evoked uniform flow, sorption-desorption kinetics and species transport by convection and/or diffusion. Although the later has been neglected [18]-[22], diffusion can indeed be influential inside large equipments, thus justifying its modeling [23]. Like time-dependent 1-D BAC models, species concentrations in SFE have been assumed as $\phi = \phi(z,t)$ and $\theta = \theta(z,t)$ respectively in fluid and solid phases, so that governing PDEs have been expressed as:

$$\frac{\partial \phi}{\partial t} + v_z \frac{\partial \phi}{\partial z} = D_z \frac{\partial^2 \phi}{\partial z^2} - \frac{1-\epsilon}{\epsilon} \dot{r} \quad (5)$$

$$\frac{\partial \theta}{\partial t} = \dot{r} = \frac{1}{t_i} \left(\frac{\phi}{k_p} - \theta \right) \quad , \quad t_i = \mu \frac{l_p^2}{D_i} \quad (6)$$

While v_z , D_z and ϵ have the same meaning as in BAC equations, k_p is a partition coefficient and t_i is

an intra-particle diffusion reference time evaluated from particle features, namely, shape coefficient μ , characteristic length l_p and intra-particle diffusivity D_i . If θ_{\max} is bed maximum extraction capacity, one may impose the following initial conditions:

$$\text{at } t = 0: \phi = 0 \text{ and } \theta = \theta_{\max} \quad (7)$$

while boundary conditions can be:

$$\text{at } z = 0: \phi = 0 \quad ; \quad \text{at } z = L: \frac{\partial \phi}{\partial z} = 0 \quad (8)$$

While BAC and SFE are distinct processes, their model frameworks are quite similar to each other. As one may realize, governing PDEs for fluid-phase concentration ϕ are basically the same, apart from the fact that the sorption-desorption term \dot{r} refers to different PDEs for the solid-phase concentration θ . Aiming at preliminary LBM simulations for BAC and SFE processes, this work attempts to profit from the aforesaid similarity between model equations.

2.2 LBM fundamentals

The underlying concept of LBM is to replace the knowledge about each constituent particle (in terms of position and velocity) by a suitable description of their overall effect through a distribution function $f = f(\vec{r}, \vec{c}, t)$. Obeying Boltzmann's equation, such function f gives the probability of finding, at time t , particles about position \vec{r} with speeds within \vec{c} and $\vec{c} + d\vec{c}$. Once f becomes known, one may then assess macroscopic properties of interest [9]. In the absence of external forces, Boltzmann's equation is written as the following advection equation with a source (or sink) term:

$$\frac{\partial f}{\partial t} + \vec{c} \cdot \vec{\nabla} f = \Omega(f) = \frac{1}{\tau} (f^{\text{eq}} - f) \quad (9)$$

where the collision operator $\Omega = \Omega(f)$ gives the variation rate of function f due to collisions between particles. In the above equation, the so-called BGK (Bhatnagar-Gross-Krook) approach was evoked so as to linearize such operator as $\Omega(f) = (f^{\text{eq}} - f)/\tau$, where τ is referred to as relaxation time and f^{eq} is the local equilibrium distribution function [24].

In LBM, Eq. (9) is discretized along pre-defined lattice links (directions). Distances Δz_k separating adjacent lattice sites are discrete (subscript k refers to a given link) and so is time, so that Δt is a discrete advancing time step. Lattice arrays are identified as

$DnQm$, where n is the problem dimension (e.g., $n = 1$ for 1-D problems) while m is the number of lattice links (= number of distribution functions f_k to be solved). Entailing a central site and two neighbors, Fig. 3 sketches a 1-D lattice array known as D1Q3, which is similar to D1Q2. Through the lattice links connecting the central site to its neighbors, particles may then "stream" with either forward or backward velocities, $\vec{c}_1 = +c \hat{z}$ or $\vec{c}_2 = -c \hat{z}$ ($c = \Delta z/\Delta t =$ lattice speed, $\hat{z} =$ unit vector), as Fig. 3 suggests. Central velocity is null, i.e., $c_0 = 0$.

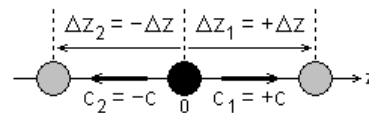


Fig. 3. Either D1Q2 or D1Q3 lattice arrays for one-dimensional (1-D) LBM simulations.

Two usual 2-D lattice arrays are shown in Fig. 4. Including the null velocity at the central site, D2Q5 array comprises 5 lattice speeds \vec{c}_k ($k = 0, 1, 2, 3, 4$) but it cannot be used for flow simulations [3] so that D2Q9 array should be used instead, which entails 5 lattice speeds \vec{c}_k ($k = 0, 1, \dots, 7, 8$).

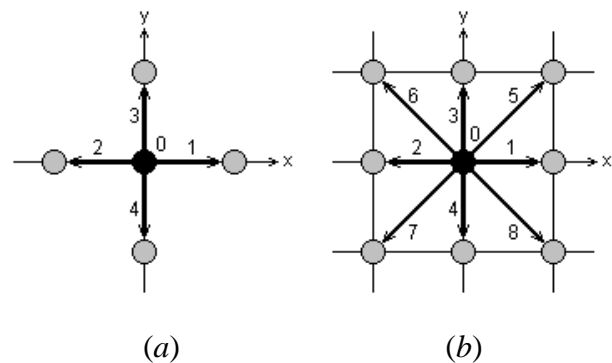


Fig. 4. (a) D2Q5 and (b) D2Q9 lattice arrays for two-dimensional (2-D) LBM simulations.

With solid lines representing lattice links, Fig. 5 shows two common 3-D arrays: D3Q15 and D3Q19. There are 15 lattice speeds \vec{c}_k ($k = 0, 1, \dots, 13, 14$) in the former and 19 lattice speeds \vec{c}_k ($k = 0, 1, \dots, 17, 18$) in the later.

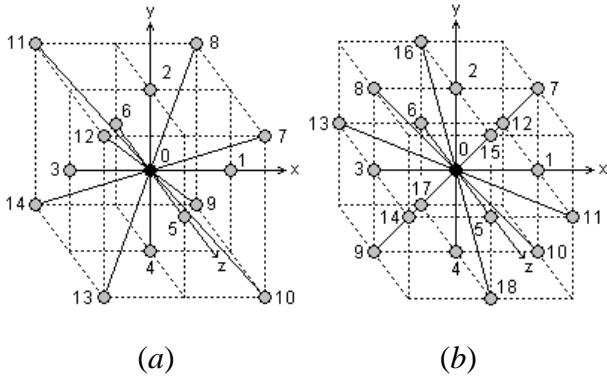


Fig. 5. (a) D3Q15 and (b) D3Q19 lattice arrays for three-dimensional (3-D) LBM simulations.

By writing Eq. (9) for a direction k at a position z and time t , one then obtains 1-D lattice-Boltzmann equation under BGK approach, namely:

$$\frac{\partial f_k(z,t)}{\partial t} + c_k \frac{\partial f_k(z,t)}{\partial z} = \frac{f_k^{eq}(z,t) - f_k(z,t)}{\tau} \quad (10)$$

where $c_k = \Delta z_k / \Delta t$ ($\Delta z_k = \pm \Delta z$, depending on the streaming direction). For D1Q3 arrays, Eq. (10) is written for $k = 0, 1$ and 2 (i.e., for f_0, f_1 and f_2) while for D1Q2 arrays it is only written for $k = 1$ and 2 as function f_0 ($k = 0$) is disregarded.

Space-time discretization of Eq. (10) renders the following algebraic equation (the order of left-hand side terms has been changed for aesthetic purposes):

$$c_k \frac{f_k(z + \Delta z_k, t + \Delta t) - f_k(z, t + \Delta t)}{\Delta z_k} + \frac{f_k(z, t + \Delta t) - f_k(z, t)}{\Delta t} = \frac{f_k^{eq}(z, t) - f_k(z, t)}{\tau} \quad (11)$$

By introducing the so-called relaxation parameter $\omega = \Delta t / \tau$, the previous equations is rewritten as:

$$f_k(z + \Delta z_k, t + \Delta t) = [1 - \omega] f_k(z, t) + \omega f_k^{eq}(z, t) \quad (12)$$

whose evolution is carried out in two steps [3]. In the collision step (= time evolution), distribution functions f_k for each direction k are updated at each lattice site from instant t to $t + \Delta t$ as:

$$f_k(z, t + \Delta t) = [1 - \omega] f_k(z, t) + \omega f_k^{eq}(z, t) \quad (13)$$

In the streaming step (= spatial evolution), collision results are transported to adjacent sites according to:

$$f_k(z + \Delta z_k, t + \Delta t) = f_k(z, t + \Delta t) \quad (14)$$

In LBM, distinct systems can be simulated by suitably handling the relaxation parameter ω and the equilibrium distribution function f^{eq} . While the later governs the transport phenomenon (i.e., of mass, momentum or energy), the former dictates the related coefficient (i.e., mass diffusivity, kinematic viscosity or thermal diffusivity).

For mass transport, diffusivity D_z depends on ω as well as on the so-called lattice sound speed c_s as:

$$\frac{1}{\omega} = \frac{D_z}{c_s^2 \Delta t} + \frac{1}{2} \Leftrightarrow D_z = c_s^2 \left(\frac{1}{\omega} - \frac{1}{2} \right) \Delta t \quad (15)$$

where the so-called lattice sound speed is assessed as $c_s = c = \Delta z / \Delta t$ for both D1Q2 and D1Q3 arrays [3]. For either D2Q4 or D2Q5 arrays it becomes $c_s = c / \sqrt{2}$ and for D2Q9, D3Q15 or D3Q19 arrays it is $c_s = c / \sqrt{3}$. For fluid flow problems, expression for kinematic viscosity ν is similar to the previous equation by simply replacing D_z for ν whereas for heat transfer one must then replace D_z by thermal diffusivity α [3],[9].

As cited, the equilibrium distribution function f^{eq} is defined according to the transport phenomenon to be simulated. Being ϕ the transported quantity, the following expression applies for relatively low fluid flow velocities \vec{v} [3],[9]:

$$f_k^{eq} = w_k \phi \left[1 + \frac{(\vec{c}_k \cdot \vec{v})}{c_s^2} + \frac{(\vec{c}_k \cdot \vec{v})^2}{2c_s^4} - \frac{(\vec{v} \cdot \vec{v})}{2c_s^2} \right] \quad (16)$$

w_k being weighting factors satisfying the condition $\sum w_k = 1$. In the D2Q1 array, for example, $w_0 = 0$ refers to the central site while $w_1 = w_2 = 1/2$ refers to each streaming direction (Fig. 3).

Last but not least, at any position z and instant t , one may retrieve the transported quantity $\phi = \phi(z, t)$ from the distribution functions as [3],[9]:

$$\phi(z, t) = \sum_k f_k(z, t) \quad (17)$$

3 Numerical method

3.1 Dimensionless formulation

One may benefit from the similarity between BAC and SFE model equations to implement preliminary LBM simulators. In view of that, this work applies

LBM only to the species concentration ϕ in the fluid phase so that simplified forms of Eqs. (1) and (5) are considered by ignoring the source or sink term \dot{r} . Hence, an identical governing PDE for ϕ is then obtained for both BAC and SFE, namely:

$$\dot{r} = \frac{\partial \theta}{\partial t} = 0 \Rightarrow \frac{\partial \phi}{\partial t} + v_z \frac{\partial \phi}{\partial z} = D_z \frac{\partial^2 \phi}{\partial z^2} \quad (18)$$

Aiming at a dimensionless formulation of such “mutual” equation, dimensionless variables for the fluid-phase species concentration ϕ , time t and axial coordinate z are introduced as:

$$\Phi = \frac{\phi}{\phi_{\text{ref}}}, \quad T = \frac{t}{\Delta t}, \quad Z = \frac{z}{\Delta z} \quad (19)$$

where $\phi_{\text{ref}} \neq 0$ can be identified to any reference concentration while Δt and Δz were introduced in the previous section. By recalling that $c_s = c = \Delta z / \Delta t$ and $v_z = v$ for 1-D problems, Eq. (18) can then be cast into the following dimensionless form:

$$\frac{\partial \Phi}{\partial T} + \text{Ma} \frac{\partial \Phi}{\partial Z} = \frac{1}{\text{Pe}_m} \frac{\partial^2 \Phi}{\partial Z^2} \quad (20)$$

where Ma and Pe_m are lattice-based Mach and mass-transfer Péclet numbers, respectively defined as:

$$\text{Ma} = \frac{v}{c_s} = \frac{v \Delta t}{\Delta z}, \quad \text{Pe}_m = \frac{c \Delta z}{D_z} = \frac{(\Delta z)^2}{\Delta t D_z} \quad (21)$$

In order to solve Eq. (20), one may impose the following initial condition on Φ :

$$\text{at } T = 0: \quad \Phi = 0 \quad (22)$$

as well as the following boundary conditions:

$$\text{at } Z = 0 \text{ (inlet): } \quad \Phi = 1 \quad (23)$$

$$\text{at } Z = N_z = L / \Delta z \text{ (outlet): } \quad \frac{\partial \Phi}{\partial Z} = 0 \quad (24)$$

where $N_z + 1$ is the number of lattice sites, end points included. In Eq. (23), reference concentration was identified to the non-null inlet concentration ($\phi_{\text{ref}} = \phi_{\text{in}}$) in line with BAC. Without loss of generality, one may instead identify it to the non-null maximum concentration ($\phi_{\text{ref}} = \phi_{\text{max}}$) in line with SFE.

3.2 Preliminary LBM for BAC and SFE

In order to implement LBM simulators for BAC and SFE, one actually needs two distinct distribution functions $f_k(z, t)$ and $s_k(z, t)$, “sharing” the same lattice and respectively referring to species concentration in fluid and solid phases. Given the underlying physics of governing PDEs, Eqs. (1), (2), (5) and (6) (namely, diffusion-convection in fluid phase and stationary solid medium), the following equilibrium distribution functions f_k and s_k can be adopted [3]:

$$f_k^{\text{eq}}(z, t) = w_k \phi(z, t) [1 \pm v_z / c] \quad (25)$$

$$s_k^{\text{eq}}(z, t) = w_k \phi(z, t) \quad (26)$$

where the sign of v_z / c depends on the streaming direction. In line with the lattice array (but always fulfilling the condition $\sum w_k = 1$), weighting factors w_k are the same for f_k^{eq} and s_k^{eq} [3]. Yet, relaxation factors ω_f and ω_s are different for each phase:

$$\text{fluid phase } (D_z \neq 0): \quad \frac{1}{\omega_f} = \frac{D_z}{c \Delta z} + \frac{1}{2} \quad (27)$$

$$\text{solid phase } (D_z = 0): \quad \omega_s = 2 \quad (28)$$

As a first step towards LBM simulations of BAC and SFE, LBM was applied only for the fluid-phase concentration, in view of the “common” governing PDE, Eq. (20). D1Q2 array was employed so that weighting factors are $w_1 = w_2 = 1/2$. With respect to the equilibrium distribution function and to the dimensionless species concentration, the following expressions hold (for $k = 1$ or 2):

$$f_k^{\text{eq}}(Z, T) = w_k \Phi(Z, T) [1 \pm \text{Ma}] \quad (29)$$

$$\Phi(Z, T) = \sum_k f_k(Z, T) \quad (30)$$

With the help of Eqs. (21) and (27), one may write the relaxation factor as:

$$\frac{1}{\omega_f} = \frac{1}{\text{Pe}_m} + \frac{1}{2} \quad (31)$$

With respect to the initial condition (at $T = 0$), one may evoke Eq. (22) so as to impose

$$f_1(Z, 0) = w_1 \Phi(Z, 0) \quad (32)$$

$$f_2(Z,0) = w_2 \Phi(Z,0) \quad (33)$$

At bed inlet, one obtains the boundary condition for $f_2(0,T)$ via streaming from the adjacent site $f_2(1,T)$, thus $f_1(0,T)$ remains the only unknown. By imposing $\Phi(0,T) = 1$ as given by Eq. (23), one may use Eq. (30) to yield the following condition for f_1 at $Z = 0$:

$$f_1(0,T) = 1 - f_2(0,T) \quad (34)$$

Approximating $\partial\Phi/\partial Z = 0$ in Eq. (24) via first-order finite differences, the following boundary conditions are obtained for f_1 and f_2 at bed outlet ($Z = N_z$):

$$f_1(N_z, T) = f_1(N_z - 1, T) \quad (35)$$

$$f_2(N_z, T) = f_2(N_z - 1, T) \quad (36)$$

4 Results and discussion

Relying on BGK-D1Q2 approach, the present work programmed LBM in Fortran (standard 90/95) so as to simulate time-dependent 1-D species transfer as governed by Eq. (20) subjected to Eqs. (22), (23), (24). Resulting from the numerical implementation of streaming and collision steps, LBM codes follow those encountered in [4] for transport phenomena of similar nature. The proposal here is to check out the proper implementation of LBM codes as regards to species concentration in fluid phase. Parameter N_z was set to yield 151 sites (end points included).

For the sake of comparison, a finite-differences method (FDM) code was equally implemented with 151 grid points (end points included). With respect to how Eq. (20) is discretized in such FDM code, it is worth remarking that:

- Time derivative $\partial\Phi/\partial T$ was discretized via first-order forward differences while explicit formulation was used for the remaining terms. Instabilities were indeed observed for $\Delta T > 0.3$ so that such scheme should be replaced by either a fully or partially implicit scheme [25],[26]. In contrast, no restrictions on the advancing time step ΔT must be imposed for LBM simulations.
- Convective term $\partial\Phi/\partial Z$ was discretized by means of upwind scheme, which may yield false (numerical) diffusion. Particularly noted ahead for lower D_z , such effect may explain why gradients in FDM profiles are “smoother” when compared to LBM counterparts.

Profiles for Φ simulated at $T = 600$ via LBM and FDM are compared in Fig. 6 for some distinct Pe_m

values with $Ma = 0.1$. Bearing in mind, for instance, a bed length $L = 0.075$ m and an interstitial velocity $v_z = 0.0002$ m/s (i.e., laboratory scale), such Pe_m and Ma values then yield $\Delta z = 0.0005$ m and $\Delta t = 0.25$ s (thus, $T = 600$ renders $t = 300$ s) while they may refer to the following values for species diffusivity D_z and relaxation factor ω_f :

- $Pe_m = 0.8 \Rightarrow D_z = 1.25 \times 10^{-6}$ m²/s and $\omega_f = 4/7$;
- $Pe_m = 4.0 \Rightarrow D_z = 2.50 \times 10^{-7}$ m²/s and $\omega_f = 4/3$;
- $Pe_m = 8.0 \Rightarrow D_z = 1.25 \times 10^{-7}$ m²/s and $\omega_f = 8/5$.

(Many other combinations are obviously feasible by assuming distinct values for L and v_z).

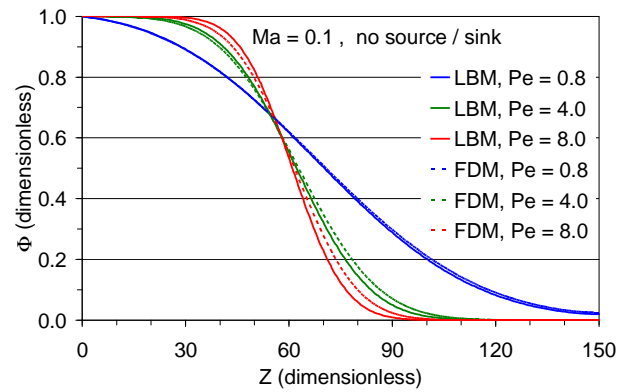


Fig. 6. LBM and FDM simulations of Φ profiles at $T = 600$ using $Ma = 0.1$ (fixed) and $Pe_m = 0.8, 4$ or 8 : diffusive-convective transport.

Despite LBM and FDM simulators were able to reproduce expected Φ profiles, differences between numerical results become apparent as Pe_m increases or, in view of Eq. (21), as v_z (convection) increases with regard to D_z (diffusion). One might assign such differences to false diffusion in FDM.

In effect, further comparisons between LBM and FDM simulations were carried out by neglecting the convective term in Eq. (20), i.e., by setting $Ma = 0$. A diffusion-dominant PDE for the dimensionless concentration Φ in the fluid phase is obtained:

$$\frac{\partial\Phi}{\partial T} = \frac{1}{Pe_m} \frac{\partial^2\Phi}{\partial Z^2} \quad (37)$$

Moreover, by imposing $v_z = 0$ in Eq. (29), fluid-phase equilibrium distribution functions become analogous to solid-phase counterparts, Eq. (30). One may then write (in dimensionless form):

$$f_k^{eq}(Z,T) = w_k \Phi(Z,T) \quad , \quad k = 1, 2 \quad (38)$$

Also subjected to boundary and initial conditions as given by Eqs. (32), (33), (34), (35) and (36), Eq. (37) was solved via LBM and FDM. Resulting Φ profiles simulated at $T = 600$ are compared in Fig. 7. In the absence of the convective term (and of false diffusion), it is worth observing that LBM and FDM profiles are practically coincident for each Pe_m .

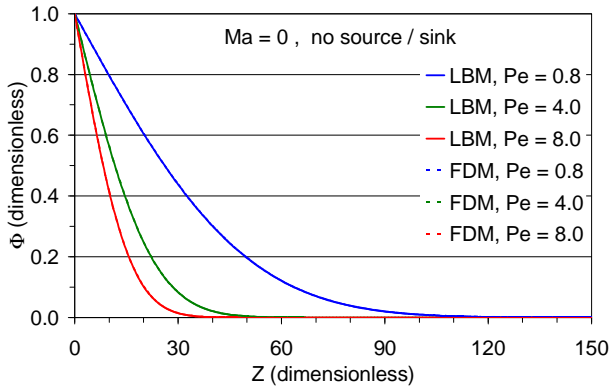


Fig. 7. LBM and FDM simulations of Φ profiles at $T = 600$ using $Ma = 0$ (fixed) and $Pe_m = 0.8, 4$ or 8 : diffusion-only (convective transport neglected).

Additional comparisons between LBM and FDM simulations were accomplished by adding a constant term \dot{R} into the right-hand side of Eq. (37) as:

$$\frac{\partial \Phi}{\partial T} = \frac{1}{Pe_m} \frac{\partial^2 \Phi}{\partial Z^2} + \dot{R} \quad , \quad \dot{R} = \frac{\dot{r} \Delta t}{\phi_{ref}} \quad (39)$$

In view of Eqs. (1) and (5), one may interpret it as an attempt to account for the presence of the solid phase. From the fluid phase standpoint, such new term in Eq. (39) behaves as a source in SFE ($\dot{R} > 0$) or as a sink in BAC ($\dot{R} < 0$). In LBM, one inserts sources or sinks in the right-hand side of Eq. (9) so that the collision step is extended to [3]:

$$f_k(Z, T + \Delta T) = [1 - \omega_f] f_k(Z, T) + \omega_f f_k^{eq}(Z, T) + w_k \dot{R} \Delta T \quad (40)$$

where weighting factors are again $w_1 = w_2 = 1/2$.

Also subjected to boundary and initial conditions as imposed by Eqs. (32), (33), (34), (35) and (36), with $\dot{R} = 0.01$ as a source term, Eq. (39) was solved via LBM and FDM. Advancing time steps were $\Delta T = 1.0$ for LBM and $\Delta T = 0.3$ for FDM so as to avoid numerical instabilities. Simulated Φ profiles at $T = 600$ are shown in Fig. 8 where one notes that LBM

and FDM results are practically coincident for each Pe_m . While it is worth recalling that Eq. (39) lacks a convective term (thus false diffusion is absent), one verifies that both simulators were able to reproduce the expected influence of the source term.

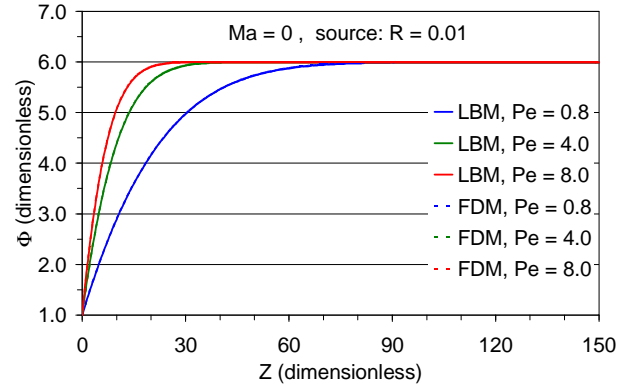


Fig. 8. LBM and FDM simulations of Φ profiles at $T = 600$ using $Ma = 0$ (fixed) and $Pe_m = 0.8, 4$ or 8 : diffusion-only with source term.

In order to examine prospective false diffusion effects together with those from the source term, further comparisons between LBM and FDM were carried out by solving the following PDE for the dimensionless fluid-phase concentration:

$$\frac{\partial \Phi}{\partial T} + Ma \frac{\partial \Phi}{\partial Z} = \frac{1}{Pe_m} \frac{\partial^2 \Phi}{\partial Z^2} + \dot{R} \quad (41)$$

Such previous PDE becomes a dimensionless form of either Eq. (1) or (5) provided that the source or sink term \dot{R} is suitably modeled in line with BAC or SFE processes (which evokes the solution of the related PDE for the solid-phase concentration).

Also subjected to the same boundary and initial conditions, Eqs. (32), (33), (34), (35) and (36), Eq. (41) was solved with $\dot{R} = 0.01$ as a source term and $\Delta T = 1.0$ and $\Delta T = 0.3$ as advancing time steps for LBM and FDM, respectively. Simulated Φ profiles at $T = 600$ are shown in Fig. 9, where false diffusion effects in FDM results can be once again identified, yet relatively to minor extent if compared to those in Fig. 6. As expected, false diffusion effects become more evident for higher Pe_m (higher convection in relation to diffusion), together with the “sweeping” effect of the percolating fluid flow, when compared to counterpart profiles in Fig. 8.

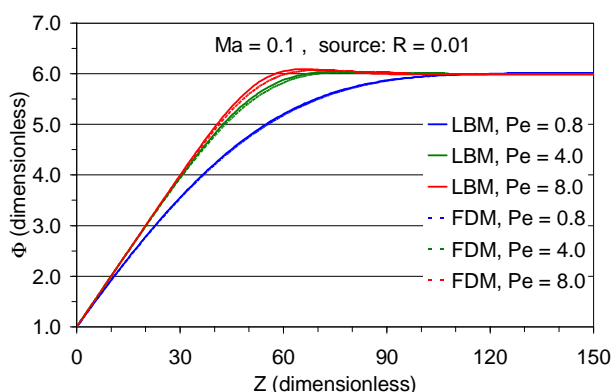


Fig. 9. LBM and FDM simulations of Φ profiles at $T = 600$ using $Ma = 0.1$ (fixed) and $Pe_m = 0.8, 4$ or 8 : diffusion-convection with source.

5 Concluding remarks

As far as species concentration in the fluid phase is concerned, time-dependent 1-D equations for BAC or SFE processes in fixed beds are so similar that one is able to arrive at the same governing PDE by neglecting each related sorption-desorption term. Profiting from such likeness, this work implemented preliminary LBM simulators for either BAC or SFE, by starting from such mutual equation and casting it into dimensionless form. FDM simulators were also implemented for comparison purposes in terms of numerical validity and performance.

Dimensionless concentration profiles simulated through LBM and FDM were practically coincident as regards to the common governing PDE as well as with respect to variations of it, namely, diffusion-dominant scenario (i.e., convection neglected) and inclusion of a source term. It is then believed that differences noted between LBM and FDM profiles can be assigned to false (i.e., numerical) diffusion effects attributable to the upwind (i.e., first-order) discretization of convective term in FDM. Besides, LBM simulations proved to be exempt from the well-known numerical stability criteria that must be obeyed by FDM simulations when the later rely on an explicit scheme with respect to time.

Those previous results are encouraging having in mind the ability to deal with more comprehensive simulations of both BAC and SFE processes in fixed beds. A primary objective is to widen each model framework in order to include the PDE for species concentration in the solid phase. Other extensions include 2-D (or 3-D) domains and the inclusion of additional transport phenomena (e.g., heat transfer and/or bed hydrodynamics).

Acknowledgement

The author thanks FAPESP (São Paulo Research Foundation, Brazil) for their financial support to the research project (No. 05/02538-1) from which the present work derives.

Nomenclature

A	cross-sectional area (m^2)
c	lattice speed ($m \cdot s^{-1}$)
D	species (mass) diffusivity ($m^2 \cdot s^{-1}$)
f	distribution functions (dimensionless)
k_p	partition coefficient (dimensionless)
k_1	sorption constant (suitable units)
k_2	desorption constant (suitable units)
L	length of the fixed bed (m)
l_p	particle characteristic length (m)
Ma	Mach number (dimensionless)
N_z	last site/grid point index (dimensionless)
Pe_m	(mass) Péclet number (dimensionless)
R	inner radius of the fixed bed (m)
\dot{R}	dimensionless source or sink term
r	lattice position (m)
\dot{r}	source or sink term (suitable units)
s	distribution function (dimensionless)
T	dimensionless time
t	time (s)
\dot{V}	volumetric flow rate ($m^3 \cdot s^{-1}$)
v	fluid velocity ($m \cdot s^{-1}$)
w	weighting factors (dimensionless)
Z	dimensionless axial coordinate
z	axial coordinate of the fixed bed (m)

Greek symbols

ε	fixed bed porosity (dimensionless)
Φ	dimensionless fluid-phase concentration
ϕ	fluid-phase concentration (suitable units)
μ	shape coefficient (dimensionless)
θ	solid-phase concentration (suitable units)
τ	relaxation time (s)
Ω	collision operator (s^{-1})
ω	relaxation parameter (dimensionless)

Subscripts and superscripts

eq	equilibrium distribution function
f	fluid phase
i	intra-particle diffusion coefficient/time
in	bed inlet
k	lattice direction
max	maximum adsorption/extraction capacity
ref	non-null reference concentration
s	solid phase or lattice sound speed
z	axial coordinate of the fixed bed
0	central lattice site

- 1 forward (1-D) lattice direction ()
 2 backward (1-D) lattice direction ()
 ~ seepage velocity
 ^ unit vector

Acronyms

- BAC Biospecific affinity chromatography
 D*Q* Lattice arrangements (arrays)
 FDM Finite-difference method
 LBM Lattice-Boltzmann method
 SFE Supercritical fluid extraction

References:

- [1] Gershenfeld N., *The Nature of Mathematical Modeling*, Cambridge University Press, 1999.
- [2] Datta A.K., Sablani S.S., *Mathematical modeling techniques in food and bioprocess: an overview*. In: *Handbook of Food and Bioprocess Modeling Techniques*, Sablani S.S., Rahman M.S., Datta A.K., Mujumdar A.R. (editors), CRC Press, 2007, pp. 1-11.
- [3] Mohamad A.A., *Applied Lattice Boltzmann Method for Transport Phenomena, Momentum, Heat and Mass Transfer*, University of Calgary, 2007.
- [4] Romano V.R., Foreword, *Journal of Food Engineering*, vol. 71, 2005, pp. 231-232.
- [5] Norton T., Sun D.-W., An overview of CFD applications in the food industry. In: *Computational Fluid Dynamics in Food Processing*, Sun D.-W. (editor), CRC Press, 2007, pp. 1-41.
- [6] Wang L., Sun D.-W., Recent developments in numerical modelling of heating and cooling processes in the food industry - a review. *Trends in Food Science and Technology*, vol. 14, 2003, pp. 408-423.
- [7] Wolf-Gladrow D.A., *Lattice-Gas Cellular Automata and Lattice Boltzmann Models: an Introduction*, Springer, 2000.
- [8] Succi S., *The Lattice Boltzmann Equation for Fluid Dynamics and Beyond*, Oxford University Press, 2001.
- [9] van der Sman R.G.M., Lattice Boltzmann Simulation of Microstructures, In: *Handbook of Food and Bioprocess Modeling Techniques*, Sablani S.S., Rahman M.S., Datta A.K., Mujumdar A.R. (editors), CRC Press, 2007, pp. 15-39.
- [10] Nield D.A., Bejan A., *Convection in Porous Medium*, Springer-Verlag, 1999.
- [11] Chase H.A., Prediction of the performance of preparative affinity chromatography, *Journal of Chromatography*, vol. 297, 1984, pp. 179-202.
- [12] Cowan G.H., Gosling I.S., Laws J.F., Sweeteham W.P., Physical and mathematical modeling to aid scale-up of liquid chromatography, *Journal of Chromatography*, vol. 363, 1986, pp. 37-56.
- [13] Sridhar P., Sastri N.V.S., Modak J.M., Mukherjee A.K., Mathematical simulation of bioseparation in an affinity packed column, *Chemical Engineering Technology*, vol. 17, 1994, pp. 422-429.
- [14] Kempe H., Axelsson A., Nilsson B., Zacchi G., Simulation of chromatographic processes applied to separation of proteins, *Journal of Chromatography A*, vol. 846, 1999, pp. 1-12.
- [15] Leickt L., Månsson A., Ohlson S., Prediction of affinity and kinetics in biomolecular interactions by affinity chromatography, *Analytical Biochemistry*, vol. 291, 2001, pp. 102-108.
- [16] Özdural A.R., Alkan A., Kerkhof P.J.A.M., Modeling chromatographic columns: non-equilibrium packed-bed adsorption with non-linear adsorption isotherm, *Journal of Chromatography A*, vol. 1041, 2004, pp. 77-85.
- [17] Yun J., Lin D.-Q., Yao S.-J., Predictive modeling of protein adsorption along the bed height by taking into account the axial nonuniform liquid dispersion and particle classification in expanded beds, *Journal of Chromatography A*, vol. 1095, 2005, pp. 16-26.
- [18] Sovová H., Rate of the vegetable oil extraction with supercritical CO₂ - I. Modeling of extraction curves, *Chemical Engineering Science*, vol. 49, 1994, pp. 409-414.
- [19] Reverchon E., Mathematical modeling of supercritical extraction of sage oil, *AIChE Journal*, vol. 42, 1996, pp. 1765-1771.
- [20] França L.F., Meireles M.A.A., Modeling the extraction of carotene and lipids from pressed palm oil (*Elaeis guineensis*) fibers using supercritical CO₂, *Journal of Supercritical Fluids*, vol. 18, 2000, pp. 35-47.
- [21] Wu W., Hou Y., Mathematical modeling of extraction of egg yolk oil with supercritical CO₂, *Journal of Supercritical Fluids*, vol. 19, 2001, pp. 149-159.
- [22] Lucas S., Calvo M.P., García-Serna J., Palencia C., Cocero M.J., Two-parameter model for mass transfer processes between solid matrixes and supercritical fluids: analytical solution, *Journal of Supercritical Fluids*, vol. 41, 2007, pp. 257-266.
- [23] Gaspar F., Lu T., Santos R., Al-Duri B., Modelling the extraction of essential oils with compressed carbon dioxide, *Journal of*

- Supercritical Fluids*, vol. 25, 2003, pp. 247-260.
- [24] Qian Y.H., D'Humières D., Lallemand P., Lattice BGK models for Navier-Stokes equation, *Europhysics Letters*, vol. 17, 1992, pp. 479-484.
- [25] Patankar S.V., *Numerical Heat Transfer and Fluid Flow*, Hemisphere, 1980.
- [26] Ferziger J.H., Peric M., *Computational Methods for Fluid Dynamics*, Springer-Verlag, 2002.